Temperature-dependent Optical Transmittance of Chemically Reduced Graphene Oxide/Hydroxypropyl Cellulose Assembly

Min Young Yeo,[1] Sung Young Park,*[2] and Insik In*[1]

[1]Department of Polymer Science and Engineering, Chungju National University, Chungju 380-702, Korea

[2]Department of Chemical and Biological Engineering, Chungju National University, Chungju 380-702, Korea

(Received November 19, 2011; CL-111121; E-mail: in1@cjnu.ac.kr)

Stable dispersion of chemically reduced graphene oxide (RGO) is prepared by simple noncovalent interaction with hydroxypropyl cellulose (HPC). Prepared RGO/HPC assembly shows temperature-dependent optical modulation below or above lower critical solution temperature (LCST). Different anchoring modes of HPC chains on RGO plates might contribute to the change of LCST for RGO/HPC assembly at different HPC-to-graphene mass ratio.

Solubility is one of the most important issues of carbon-based nanomaterials such as graphene for wet process to fabricate graphene-based devices.[1] The strong van der Waals interaction between graphene plates results in their limited solubility in most solvents and can be suppressed by either covalent or noncovalent "anchoring" of small molecules or polymers on single graphene plates, resulting in stable dispersion of graphene in solution.[2]

Noncovalent anchoring of water-soluble polymers on chemically reduced graphene oxide (RGO) plates has been proven to be effective for formulating stable dispersion of RGO/polymer assembly in aqueous medium.[3] But the morphological features of RGO/polymer assembly and the interaction mechanism between polymer chains and RGO plates are not completely understood. Recent theoretical calculation shows that certain biomolecules such as L-leucine can show "spontaneous anchoring" with graphene plate through van der Waals interaction.[4]

To investigate the structural features of RGO/polymer assembly in detail, it is useful to monitor response behavior of certain stimuli-responsive polymers after assembly formation with RGO plates. Any change of response of pristine polymers before and after anchoring with RGO plates might give rich information on the interaction parameters between polymer chains and graphene plates, enabling precise molecular design for certain functional graphene/polymer assembly which is promising for many applications such as drug carriers with controlled release, bioactive agents, and functional nanocomposites.

In this study, probing of different anchoring modes of polymer chains on RGO plates is attempted by using a thermoresponsive polymer, hydroxypropyl cellulose (HPC), because the mobility of anchored HPC chains can be easily monitored and compared by measuring LCSTs of different RGO/HPC assemblies. Formulation of RGO/HPC assembly is based on totally noncovalent interaction. 1.0 or 2.0 mg of as-prepared graphene oxide (GO) through Hummer's method was completely dissolved in 20 mL of deionized water after sonication.[2c,5] Then, powdered HPC was directly added and dissolved into the above GO solution according to the RGO-to-
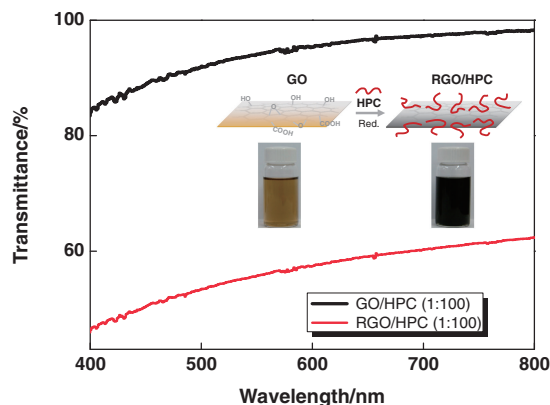

Figure 1. UV–vis spectra of GO/HPC mixture and RGO/HPC assembly solutions with the initially used GO concentration of $0.05\,\mathrm{mg\,mL^{-1}}$ and the initial feeding ratio (GO to HPC) of 1:100 at 25 °C (insets are schematic illustrations and photos for GO and RGO/HPC assembly, respectively).

HPC mass ratio (1:100, 1:50, or 1:10). Addition of hydrazine monohydrate and heating the GO/HPC mixture at 40 °C for 72 h produced dark black-colored RGO/HPC assembly solution which was optically clear and stable in all cases (Figure 1).
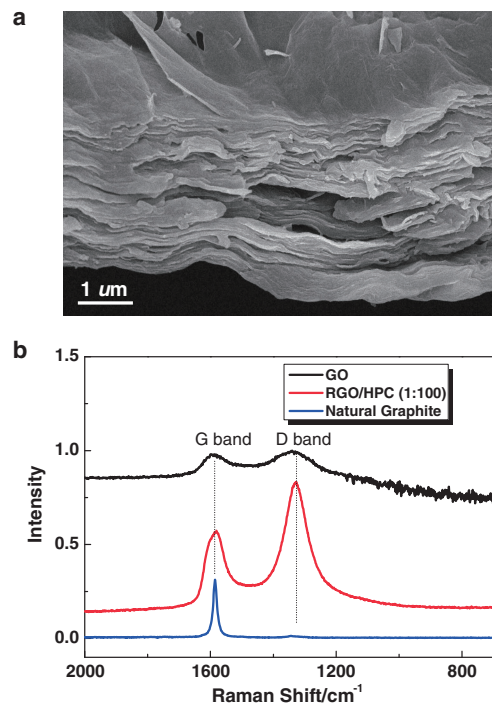
Prepared RGO/HPC assembly solutions showed different LCST behavior depending on the HPC-to-RGO feeding ratio compared with the pristine HPC which showed LCST transition around 45 °C. Dynamic light-scattering measurement of RGO/HPC (1:100) assembly solution showed both initial shrinkage on heating and final aggregation above LCST, which is typical of thermoresponsive polymers showing LCST transition.[6] The initial broad size distribution at 25 °C became narrower on heating to 40 °C and then 50 °C. At 60 °C, bigger aggregated structures started to be formed, and further heating produced precipitation. This precipitation is not aggregated RGO plates but RGO/HPC assemblies because black-colored precipitated solid was readily soluble again on cooling to 25 °C.

Next, temperature-dependent transmittance of both GO/HPC mixture and RGO/HPC assembly solutions was monitored by UV–vis spectroscopy at 600 nm (Figure 2a). LCST transition of RGO/HPC (1:100) assembly was clearly observed at 53 °C while both pure HPC and GO/HPC (1:100) mixture solutions showed LCSTs at 45 and 46 °C, respectively. This supports that there is overall and effective noncovalent anchoring of HPC chains on hydrophobic RGO plates because any noninteracting HPC chains in solution might show LCST around 45 °C. Therefore, HPC chains are regarded to be free in GO/HPC mixture solution and to be anchored on RGO plates. When the relative amount of HPC in assembly was decreased to 1:50 and
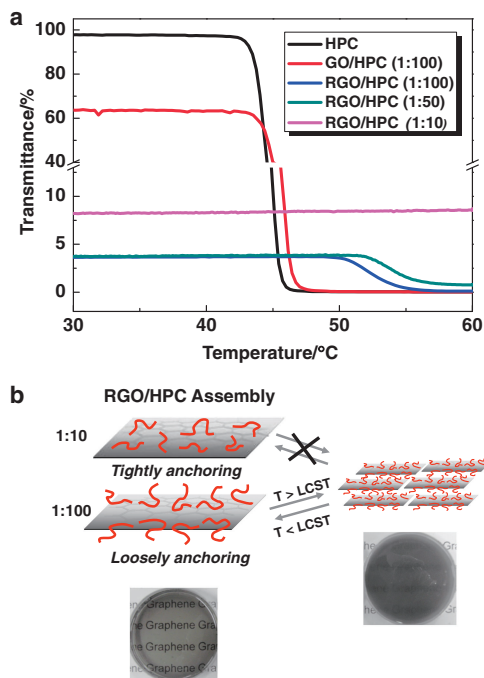
Figure 2. a) Temperature-dependent transmittance (at 600 nm) of HPC, GO/HPC, and RGO/HPC assembly solutions with the initially used GO concentration of 0.10 mg mL^{-1} and with the different RGO to HPC mass ratio and b) schematic illustration of LCST transition of RGO/HPC assemblies in different anchoring modes (inserts are photos of RGO/HPC (1:100) assembly solutions before and after LCST transition).

Figure 3. a) FE-SEM image of filtered RGO film from RGO/HPC (1:100) assembly solution and b) Raman spectra of GO, filtered RGO film (from 1:100 assembly solution), and natural graphite.

1:10, RGO/HPC assembly shows increased LCST at 55 °C in 1:50 assembly and even no LCST transition was found in 1:10 assembly. This increase of LCST in RGO/HPC assembly or disappearance of LCST transition might come from the decreased mobility of interacting HPC chains on graphene plates at lower HPC feeding ratio. Stronger noncovalent interaction force between HPC chains and RGO plates at lower HPC ratio might provide this decreased mobility between them. Then, much more energy is required for certain rearrangement of HPC chains such as shrinkage or aggregation around LCST. Therefore, higher temperature was required for LCST transition of 1:50 assembly, and even LCST transition was not observed due to much stronger interaction and resulting reduced mobility of 1:10 assembly. In addition, above thermoresponsive solubility switching of RGO/HPC assembly was quite reversible. This supports that the van der Waals interaction between HPC chains and RGO plates is robust regardless of LCST transition. Previously, we have proposed end-by-face or side-to-face orientation of anchored poly(N-isopropylacrylamide) (PNIPAM) chains on RGO plates.[3c] From the above LCST changes in RGO/HPC assemblies with different RGO-to-HPC mass ratio, it is evident that the relative amount of polymer modulates anchoring mode of polymer chains on graphene plates. Therefore, we propose here that interacting polymer chains can adopt either *loosely anchoring* mode in high polymer-to-graphene ratio or *tightly anchoring* mode in low polymer-to-graphene ratio (Figure 2b).

Further structural features of RGO/HPC were examined by AFM analysis. RGO/HPC assembly (1:100) was thicker (4–8 nm) than GO plate (typically around 1 nm). This demonstrates that HPC chains are actually interacting on graphene plates. RGO/graphene with less HPC (1:10) showed plate thickness around 2.5–3 nm.[6] This result again correlates well with previous our propose for tightly anchoring mode in low polymer-to-graphene ratio because stronger interaction might prefer end-by-face orientation which results in the decrease of overall thickness of RGO/polymer assembly. Next, solutions of RGO/HPC assembly were vacuum-filtered through anodized aluminum oxide (AAO) membrane (pore size of 200 nm), resulting in dark gray graphene only film. FE-SEM images of prepared graphene film showed typical layered film structures (Figure 3a). Raman spectra of prepared graphene film were examined and compared with those of natural graphite and GO. Filtered films show typical G and D bands at 1582 and 1328 cm^{-1}, while GO shows them at 1593 and 1341 cm^{-1} in Raman spectra (Figure 3b). For comparison, natural graphite shows only G band at 1585 cm^{-1}. In addition, the prepared graphene film shows increased D and G band intensity ratio, I(D)/I(G), compared with GO. This correlates well with the previous report by Stankovich et al., confirming that chemical reduction to graphene is successful in the presence of HPC.[2c] Interestingly, there was no noticeable peak of HPC, and this shows that most of anchored HPC chains in the RGO/HPC assembly are detached during filtration and subsequent washing. Probably, van der Waals interaction between RGO plates and HPC chains might be robust only in solution phase. While the

reason for the disconnection of van der Waals interaction between RGO and HPC in solid phase is unclear at this stage, prepared graphene film can show better electrical properties due to the absence of insulating HPC chain. Graphene film with 50% transmittance at 600 nm showed sheet resistance of 1.6×10^8 Ω/square. Calculated conductivity of this graphene film with thickness of 50 nm is $0.125 \, S \, m^{-1}$, comparable to the reported value by Eda et al.[7] This low conductivity of as-prepared RGO film can be dramatically improved by additional thermal treatment to achieve complete reduction of any residual sp^3 carbons in as-prepared RGO.

In summary, detailed interaction parameter between HPC chains and RGO plates has been explored by monitoring the change of LCST of RGO/HPC assembly with different HPC-to-RGO ratio compared with LCST of pristine HPC. Increase and further disappearance of LCST transition temperature of RGO/HPC assembly with decreasing polymer-to-RGO ratio supports that van der Waals interaction between HPC chains and RGO plates is getting stronger.

References and Notes

1 a) D. Li, M. B. Müller, S. Gilje, R. B. Kaner, G. G. Wallace, *Nat. Nanotechnol.* **2008**, *3*, 101. b) X. Fan, W. Peng, Y. Li, X. Li, S. Wang, G. Zhang, F. Zhang, *Adv. Mater.* **2008**, *20*, 4490. c) Y. Si, E. T. Samulski, *Nano Lett.* **2008**, *8*, 1679. d) J. Y. Lee, I. In, *Chem. Lett.* **2011**, *40*, 567. e) Y. M. Jo, S. Yoon, J.-H. Lee, S.-J. Park, S. R. Kim, I. In, *Chem. Lett.* **2011**, *40*, 54.

2 a) D. A. Dikin, S. Stankovich, E. J. Zimney, R. D. Piner, G. H. B. Dommett, G. Evmenenko, S. T. Nguyen, R. S. Ruoff, *Nature* **2007**, *448*, 457. b) S. Watcharotone, D. A. Dikin, S. Stankovich, R. Piner, I. Jung, G. H. B. Dommett, G. Evmenenko, S.-E. Wu, S.-F. Chen, C.-P. Liu, S. T. Nguyen, R. S. Ruoff, *Nano Lett.* **2007**, *7*, 1888. c) S. Stankovich, R. D. Piner, X. Chen, N. Wu, S. T. Nguyen, R. S. Ruoff, *J. Mater. Chem.* **2006**, *16*, 155.

3 a) S. Yoon, I. In, *J. Mater. Sci.* **2011**, *46*, 1316. b) S. Yoon, I. In, *Chem. Lett.* **2010**, *39*, 1160. c) D. Y. Lee, S. Yoon, Y. J. Oh, S. Y. Park, I. In, *Macromol. Chem. Phys.* **2011**, *212*, 336. d) D. Y. Lee, Z. Khatun, J.-H. Lee, Y.-k. Lee, I. In, *Biomacromolecules* **2011**, *12*, 336. e) J. Y. Lee, I. In, *Chem. Lett.* **2012**, *41*, 127.

4 W. Qin, X. Li, W.-W. Bian, X.-J. Fan, J.-Y. Qi, *Biomaterials* **2010**, *31*, 1007.

5 Y. Xu, H. Bai, G. Lu, C. Li, G. Shi, *J. Am. Chem. Soc.* **2008**, *130*, 5856.

6 Supporting Information is available electronically on the CSJ-Journal Web site, http://www.csj.jp/journals/chem-lett/index.html.

7 G. Eda, G. Fanchini, M. Chhowalla, *Nat. Nanotechnol.* **2008**, *3*, 270.